

## Electron-Electron Scattering at 6.1 Mev\*

W. C. BARBER, G. E. BECKER,† AND E. L. CHU

*Microwave Laboratory, Department of Physics, Stanford University, Stanford, California*

(Received June 17, 1952)

The absolute differential cross section for the scattering of 6.1-Mev electrons by the electrons in a beryllium foil has been measured at 90 degrees and 109 degrees in the center-of-mass system. Electrons from a linear accelerator were first magnetically analyzed and then collimated to form the incident beam. Electron-electron scattering events were detected by end-window Geiger counters connected in coincidence. The counter with the defining aperture was connected in coincidence (1) with a counter at the conjugate scattering-angle, lying in the plane determined by the incident beam and the scattering direction to the defining counter; and (2), with another counter at the conjugate angle, but lying outside this plane, thus counting only accidental coincidences. The number of  $e$ - $e$  coincidences was then given by the difference between (1) and (2), with appreciable corrections arising from

asymmetry in the background and from dead-time losses. These corrections required measurements of single and coincidence count rates with the scatterer in and out of the beam.

The result at 109 degrees was 4.4 percent lower than that predicted by the Møller theory, with a standard deviation based on the number of counts recorded of  $\pm 6$  percent. At 90 degrees the expected standard deviation was  $\pm 2$  percent, and here the experimental result was 8 percent below the theoretical. The latter result suggests the possibility that the Møller theory overestimates the cross section. However, consideration of the effects produced by radiative collisions, and of possible systematic errors in the experiment, leads to the conclusion that the experimental result is not incompatible with the Møller theory.

### I. INTRODUCTION

A CALCULATION of the differential cross section for electron-electron scattering was made by Møller,<sup>1</sup> using the Dirac theory. His result may be written as follows:

$$\sigma(\theta) = 2 \left( \frac{e^2}{m_0 v^2} \right)^2 \frac{\gamma + 1}{\gamma^2} \frac{(\gamma^*)^2 \cos \theta}{[\cos^2 \theta + (\gamma^*)^2 \sin^2 \theta]^2} \times \left\{ \frac{\theta^*}{2} \csc^4 \frac{\theta^*}{2} + \frac{\theta^*}{2} \sec^4 \frac{\theta^*}{2} - \frac{\theta^*}{2} \csc^2 \frac{\theta^*}{2} \sec^2 \frac{\theta^*}{2} + \left( \frac{\gamma - 1}{\gamma} \right)^2 [1 + 4 \csc^2 \theta^*] \right\}, \quad (1)$$

where  $\theta$  is the scattering angle in the laboratory system,  $\theta^*$  the corresponding angle in the center-of-mass system,  $e$ ,  $m_0$ , and  $v$  the electron charge, rest mass, and velocity, respectively,  $\gamma = 1/[1 - v^2/c^2]^{1/2} = m/m_0$ , and  $\gamma^* = [(\gamma + 1)/2]^{1/2}$ . The relationship of  $\sigma(\theta)$  to experimentally observable quantities is given by

$$\sigma(\theta) = Y/nN\Omega, \quad (2)$$

where  $Y$  is the number of scattered electrons reaching a detector at the angle  $\theta$  which subtends a small solid angle  $\Omega$  at the scatterer,  $N$  is the number of incident electrons, and  $n$  is the number of electrons per  $\text{cm}^2$  in the scatterer. A theory based on the Schrödinger equation yields the Mott<sup>2</sup> formula, which differs from (1) only in that the fourth term in the bracket is missing. The relativistic classical expression results when both the third and the fourth terms in the bracket of (1) are dropped.

Until very recently, the only experimental checks were made by studying cloud-chamber tracks.<sup>3,4</sup> All these results taken together discriminated against the classical expression, but were not sufficiently precise to show that the Møller formula was more accurate than the Mott formula. Within the last two years, experiments have been done in which counting techniques were used to obtain more precise results.<sup>5,6</sup> These experiments gave results which agreed with the Møller formula within the experimental uncertainty, and which, together with the earlier results, showed the inadequacy of all other published formulas not based on the Dirac theory.

This paper describes an experiment using electrons from a linear accelerator, with a kinetic energy of 6.1 Mev. The corresponding energy in the center-of-mass system is 0.85 Mev, assuming that the target electron is at rest in the laboratory. This energy is very suitable for a study of  $e$ - $e$  scattering since the collisions are quite relativistic, the differential cross section is large (about  $10^{-25}$   $\text{cm}^2/\text{steradian}$ ), and the laboratory scattering angles of chief interest are of a convenient magnitude.

### II. COINCIDENCE METHOD

A coincidence method may be used to distinguish electron-electron scattering from other types of scattering which occur in the foil. If an electron of momentum  $\mathbf{p}_0$  makes an elastic collision with a second electron initially at rest, the two electrons emerge with momenta  $\mathbf{p}_1$  and  $\mathbf{p}_2$ , at angles  $\theta$  and  $\phi$ , respectively (see Fig. 1). The laws of conservation of energy and momentum permit the calculation of  $\phi$ ,  $\mathbf{p}_1$ , and  $\mathbf{p}_2$ , if  $\mathbf{p}_0$  and  $\theta$  are given. The relationship between the labo-

\* Assisted in part by the joint program of the U. S. Office of Naval Research and the U. S. Atomic Energy Commission.

† Now at Hudson Laboratories, Columbia University, Dobbs Ferry, New York.

<sup>1</sup> C. Møller, *Ann. Physik* **14**, 531 (1932).

<sup>2</sup> N. F. Mott, *Proc. Roy. Soc. (London)* **A126**, 259 (1930).

<sup>3</sup> F. C. Champion, *Proc. Roy. Soc. (London)* **A137**, 688 (1932).

<sup>4</sup> Groetzinger, Leder, Ribe, and Berger, *Phys. Rev.* **79**, 454 (1950). This reference contains a review of earlier cloud-chamber work.

<sup>5</sup> L. A. Page, *Phys. Rev.* **81**, 1062 (1951).

<sup>6</sup> Scott, Hanson, and Lyman, *Phys. Rev.* **84**, 638 (1951).

ratory angles  $\theta$  and  $\phi$  is given by  $\tan\theta = [2/(1+\gamma)] \cot\phi$ , where  $\gamma = [1 - (v^2/c^2)]^{-1/2}$ ,  $v$  is the velocity of the incident electron in the laboratory, and  $c$  is the velocity of light.  $\mathbf{p}_2$  must lie in the plane determined by the vectors  $\mathbf{p}_0$  and  $\mathbf{p}_1$ . An electron detector with a defining aperture at the angle  $\theta$  connected in coincidence with another detector with a conjugate aperture at the conjugate angle  $\phi$  should count the  $e$ - $e$  events at the angle  $\theta$ . In practice, because of the finite resolving time of the coincidence circuit, there will be chance coincidences, resulting, for example, from two distinct nuclear scattering events in the foil. These chance coincidences may be measured and subtracted from the total by connecting in coincidence with the detector at  $\theta$  a third detector at the angle  $\phi$ , but lying outside the plane determined by the vectors  $\mathbf{p}_0$  and  $\mathbf{p}_1$ . It is assumed that the number of chance coincidences arising from events occurring in the scattering foil is the same for each coincidence pair. The same may not be assumed for the number of chance coincidences arising from the general background, with no scattering foil, and it is necessary to make a separate measurement of these.

Of course, it is possible to write down an expression for the expected number of accidental coincidences if the single count rates for the two counters of a coincidence pair are known. This procedure of calculating the number of accidental coincidences is less accurate than actually measuring them with a second coincidence pair, for reasons which can be better discussed below, after the apparatus has been described.

While it is true that the incident electron beam may be contaminated with x-rays which can give rise to Compton scattering or pair production in the foil, such events will not lead to a false result for the number of  $e$ - $e$  coincidences. The two photons and the electron involved in a Compton scattering process do have

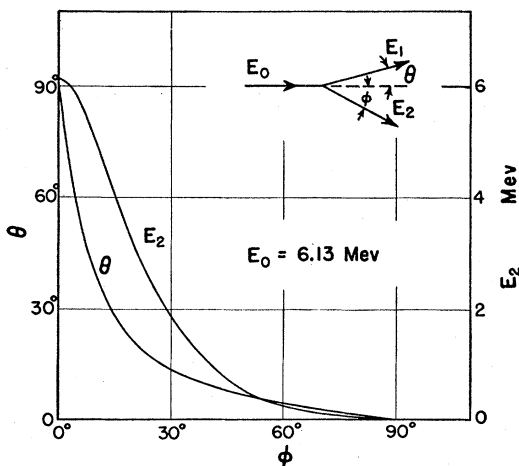


FIG. 1. One curve gives the relationship between the conjugate laboratory angles  $\theta$  and  $\phi$  for the case of an electron-electron collision, with incident electron energy = 6.1 Mev. The other curve gives the energy of the electron scattered at the angle  $\theta$  for the same case.

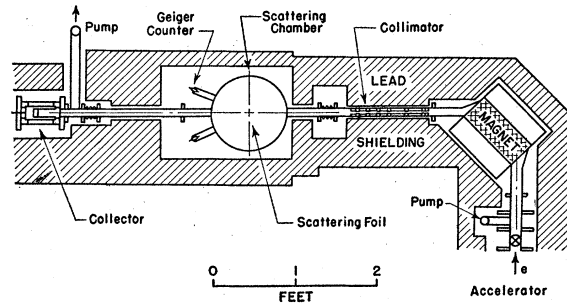


FIG. 2. Schematic diagram of the arrangement of the apparatus.

co-planar paths, but the conjugate angles after scattering are not the same as for the  $e$ - $e$  case. As for the pair production process, the probability that the angle between the positron-photon and electron-photon planes have a given value between 0 degrees and 180 degrees is almost constant as a function of angle. The slightly greater probability for angles near 180 degrees would not lead to any measurable effects in this experiment.

In order that no coincidences be missed, the conjugate aperture must be larger than the defining aperture. The reasons for this have been thoroughly presented previously,<sup>7</sup> and need not be repeated in detail here. The effects of the finite beam size and the fact that  $(d\phi/d\theta) \neq 1$  are easily taken into account. Other factors which are important in determining the required conjugate aperture size are (1) multiple scattering, (2) possible small misalignments, and (3) the initial motions of the target electrons in the foil. A first approximation to the required aperture size may be based on numerical estimates for each of these factors. But in order that one may be certain that the conjugate aperture has been made large enough, a series of measurements must be made with increasing conjugate aperture size, until the point is reached where the observed result no longer increases with conjugate aperture size.

Counting corrections which arise because of the dead time of the electron detectors will be discussed in a separate section below.

### III. APPARATUS

#### A. Beam Formation

A schematic diagram of the arrangement of the apparatus is given in Fig. 2. The electron beam from the accelerator was first passed through a  $\frac{1}{32}$ -in. cylindrical hole in a 1-in. thickness of polystyrene, and was then magnetically analyzed and collimated. The range of energies of the electrons transmitted by the magnet and collimator system was  $\pm 0.13$  Mev at an energy of 6.1 Mev. The 14-in. length of collimator consisted of  $\frac{1}{16}$ -in. cylindrical holes in aluminum and

<sup>7</sup> See, for example, Karr, Bondelid, and Mather, Phys. Rev. 81, 37 (1951).

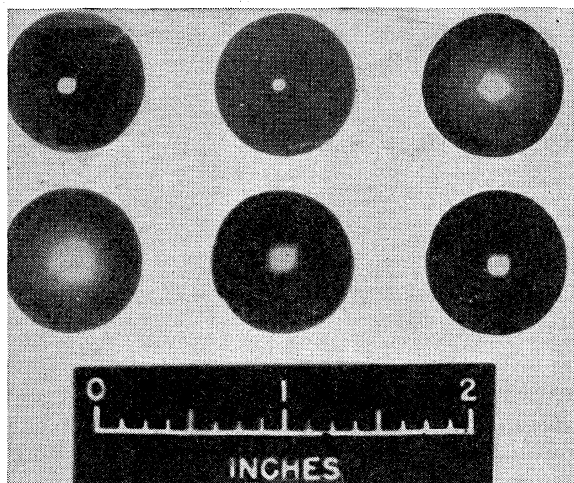


FIG. 3. Cross sections of the electron beam at various points along its path. Upper row from right to left: (1) At the entrance to the collimator tube. The horizontal spread results from the spread in energy of the electrons from the accelerator. (2) At the exit of the collimator tube. (3) At the position of the scattering foil. Lower row from right to left: (1) At the end of the exit tube of the scattering chamber. (2) At a point 4 inches in front of the collection cup. (3) Same position as for (2), but with a  $\frac{1}{4}$ -mil nylon foil scatterer.

polystyrene, separated by lead spacers with larger holes. Electrons could strike only the low  $Z$  materials, which were used to minimize bremsstrahlung.

The apparatus was first lined-up approximately with various mechanical devices. Final adjustment was made with the aid of films inserted at various points, which revealed the shape of the beam and its location with respect to the axis of the apparatus. The beam was made to coincide with this axis to within  $\pm\frac{1}{32}$  inch. Figure 3 shows the cross section of the beam at various points along its path. After collimation, the total angle of spread was 0.2 degree.

### B. Scattering Chamber

The cylindrical scattering chamber was made of brass, 12 inches in diameter, 8 inches in height, with  $\frac{1}{8}$ -in. walls. The chamber was lined with polystyrene  $\frac{3}{16}$  in. in thickness, coated with Aquadag. This was done to minimize backscattering of electrons from the walls. Thin windows in the wall at a few fixed angles served as exit ports for the scattered electrons. Figure 4 shows a view of the scattering chamber from the exit tube, giving the projection of each window on a plane perpendicular to the beam. The pairs of windows for counters lying in a plane with the incident beam are indicated by the dotted lines. On the assumption that the electron beam was correctly aligned, knowledge of the scattering angle  $\theta$  depended on the precision of the machine work in locating the holes for the windows. The various angles should be correct to within  $\pm 0.1$  degree, but no other means were devised to check this.

### C. Detectors

End-window type Geiger-Müller counters were used as detectors. Those used in the earlier stages of the experiment were made by bolting the counter cathode shells directly onto the scattering chamber. A single 0.001-inch aluminum window separated the vacuum of the scattering chamber from the counter gas, which was a mixture of argon and alcohol at a total pressure of 8 cm of mercury. The plateaus of these counters were very poor, rising 30 to 50 percent in 100 volts. However, the counter characteristics remained stable over a period of several months. The excessive rise of the plateaus was chiefly caused by multiple pulses, which would not affect the coincidence count rates appreciably. The multiple pulses produced errors in the single count rates until gating circuits were introduced to limit the sensitive time to the period when the accelerator was on. Even without the gating circuits, the errors in the single count rates produced only second-order errors in the final result.

While there was no specific reason to doubt the results obtained with these counters, it was decided to repeat the experiment, at angle  $\theta^* = 90$  degrees, using commercial (Tracerlab) mica-window counters, with good plateaus. This necessitated the use of two windows, but the separation of the windows was only  $\frac{3}{16}$  inch, and the combined window thickness did not exceed  $12 \text{ mg/cm}^2$ , so that the transmission for electrons of energy greater than 1 Mev was still essentially 100 percent. These counters were filled with helium and a quenching gas to a total pressure near one atmosphere. The  $e-e$  scattered electrons had energies in excess of 2 Mev at the angles studied in this experiment. Calculations show that, with the given geometry and window thickness, any such electron should have had a path

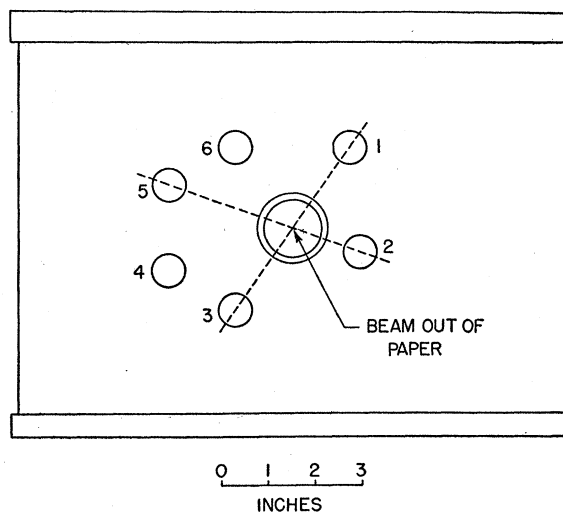


FIG. 4. A view of the scattering chamber from the exit tube, giving the approximate location of the Geiger counters. The numbered circles give the distorted projection of each counter window on a plane perpendicular to the incident beam.

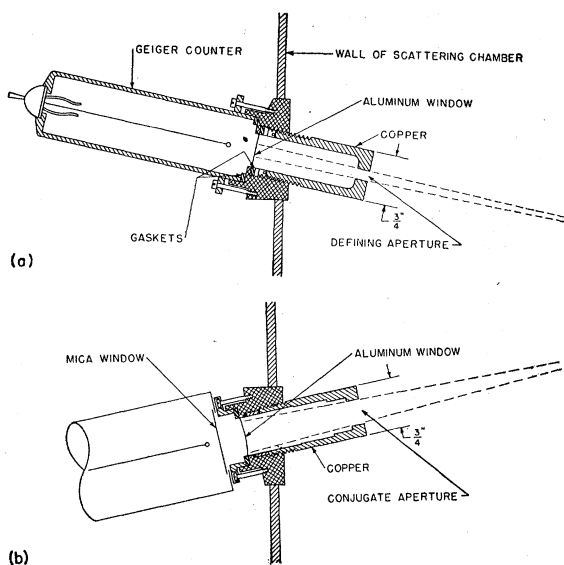


FIG. 5. Scale drawing showing the aperture determining the solid angle subtended at the scatterer. (a) A defining aperture with tapered walls is shown in front of an argon-alcohol counter with a single aluminum window. (b) A conjugate aperture is shown in front of a helium-filled (Tracerlab) counter with a mica window.

length of at least one cm within the active volume of the Geiger counter. The gas pressures in the Geiger counters were great enough to make the probability of producing one or more ions negligibly less than 100 percent under these circumstances.

At the conclusion of the experiment, a standard coincidence method<sup>8</sup> employing the sea-level cosmic radiation was used to check the efficiency of one of the Tracerlab counters. The result indicated that the efficiency is in the range of 0.975 to 1.00, but the possibility of wide angle scattering and the uncertainty of the correction for showers restricted the precision of the determination to the above limits. The result of this measurement is not inconsistent with the theoretically estimated efficiency of essentially 100 percent. This theoretical estimate has been used in calculating cross sections, but since there is no experimental proof of this point, we must allow the possibility of a systematic error.

The solid angle subtended at the foil by a detector was determined by a tapered cylindrical hole in a copper solid cylinder screwed into position in front of the Geiger counter, as shown in Fig. 5. In order to vary the aperture size, it was necessary to remove the lid of the scattering chamber and insert a new copper cylinder. The knowledge of the solid angle subtended by an aperture depended on mechanical measurements which were accurate to within  $\pm \frac{1}{2}$  percent. The fact that the axis of each copper cylinder intersected the path of the electron beam at the center of the chamber was checked by mechanical means. Any errors in the

<sup>8</sup> J. C. Street and R. H. Woodward, Phys. Rev. 46, 1029 (1934).

position of this point of intersection were found to be less than  $\frac{1}{32}$ -in.

#### D. Electronic Circuits

A block diagram of the electronic circuits is shown in Fig. 6. The gates insured that counts were registered only when the accelerator was turned on. In the early stages of the experiment, these gates were not used, and it was necessary to measure and subtract counts arising from cosmic rays and other background with the accelerator off. The resolving time of the coincidence circuits was  $2 \mu\text{sec}$ , a convenient number somewhat larger than the  $0.8\text{-}\mu\text{sec}$  pulse of electrons from the accelerator. Thus, the effective resolving time was just the length of this electron pulse.

#### E. Scattering Foil

Some preliminary tests were made with nylon and polystyrene foils, but careful measurements were made only with a beryllium scatterer. A scatterer of low  $Z$  was chosen for three reasons: (1) to minimize the ratio of electron-nuclear scattering to  $e-e$  scattering; (2) to minimize any effects arising from the binding of the target electron in the atom; and (3) to minimize multiple scattering in the foil.

Dr. H. Bradner of the Radiation Laboratory at Berkeley kindly supplied beryllium foils, each about  $0.4 \text{ mg/cm}^2$  in thickness. The actual scattering foil was made by mounting several of these on top of each other on a circular brass ring with inside diameter equal to one inch. The area and the mass of each foil could be determined within  $\pm 1$  percent. The uniformity of the final scattering foil was tested by measuring the transmission of polonium alpha-particles, which were near the end of their range, through various regions of the foil. The beam of alpha-particles was collimated to a cross-sectional area about equal to that of the electron beam used in the scattering experiment. The transmission of the alpha-beam was measured at 12 different places on the foil. The root mean square variation in thickness of the measured places from their mean value was 1.7 percent. The region near the center of the foil, where the electron beam passed, was more

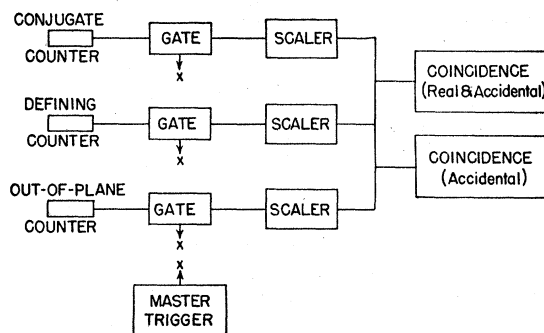


FIG. 6. Block diagram of the electronic circuits employed.

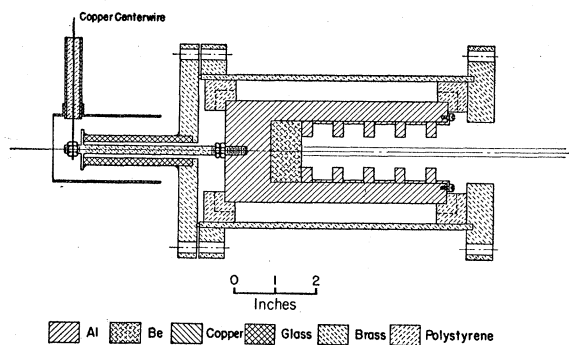


FIG. 7. Scale drawing of the current collection cup.

uniform than the foil as a whole and of thickness not appreciably different from the mean value.

After extensive measurements were made with one scatterer, it was accidentally destroyed. The measurements were repeated with an entirely new scatterer, and the observed results were unchanged. The purity of the evaporated beryllium foils was high, but was not critical in this experiment. In the light of the foregoing, we think it very unlikely that the computed number of target electrons per  $\text{cm}^2$  is in error by more than 2 percent.

#### IV. CURRENT MEASUREMENT

The average current carried by the incident electron beam was of the order of  $10^{-13}$  amp. The electrons in the beam were collected in the insulated cup shown in Fig. 7. Beryllium was used at the base of the cup to minimize bremsstrahlung and backscattering. On the basis of recently published measurements on backscattering,<sup>9</sup> and the small solid angle subtended at the base by the mouth of the cup (0.5 percent of  $2\pi$ ), it is estimated that less than 0.1 percent of the electrons could escape from the cup.

As is shown in Fig. 8, the electron current was integrated by measuring the potential across the polystyrene-insulated capacitor. The quadrant electrometer served simply as a null indicator. The electrometer deflection was held at zero by continuously adjusting the potentiometer setting during each run, so that the collector cup and associated leads were maintained at ground potential.

This procedure minimized any errors arising from ionization currents. It was shown that the application of a positive or negative bias to the collector cup could, respectively, increase or decrease the measured current by a saturation value of 3 percent from the value found with zero bias. A bias curve taken by using a Geiger counter, which measured the bremsstrahlung produced at the base of the cup, as a beam monitor is shown in Fig. 9. Because of the observed symmetry about the point of zero bias, we conclude that the ionization current is very small if the bias on the cup is zero.

<sup>9</sup> W. Bothe, Z. Naturforsch. 4a, 542 (1949).

Observations of the electrometer drift rate with the accelerator off were made before and after each run, so that corrections could be made for leakage currents. These corrections were of the order of 1 percent or less.

Once it was established that spurious effects were absent, the integration of the current depended on the potential measurement, made with an  $L$  and  $N$  potentiometer and standard cell to within  $\pm 0.1$  percent, and the value of the capacitor. This was measured at the National Bureau of Standards under dc conditions similar to those used during the experiment. The value of the capacity was found to be 0.001017 microfarad, with a stated limit of error of 0.5 percent. This determination checks with bridge measurements made at a frequency of 1000 cycles/sec.

For an over-all limit of error in the integration of the current we assign the value  $\pm 2$  percent, most of which is due to the possibility that our interpretation of the bias curve is not entirely correct.

#### V. COLLECTION OF DATA

Measurements with the foil in and out were made alternately, while every effort was made to keep all other conditions constant. In order to minimize the statistical error of the difference, approximately twice as much running time was devoted to measurements with the foil in. During a given run (typically of two hours' duration), the current was monitored and was held constant within  $\pm 10$  percent by making small adjustments in the accelerator operating conditions.

With a given set of apertures, several series of runs were taken, at different current levels. The requirement of reasonable values for the count rates limited the range of current values to a variation by a factor of 3. No systematic differences in the results at different current levels were observed.

For the case where the defining aperture was at  $\theta = 28$  degrees 4 minutes, the scattering foil was rotated 20 degrees about a vertical axis, in such a way as to reduce the path of the low energy scattered electrons in the foil. This was done to minimize multiple scattering.

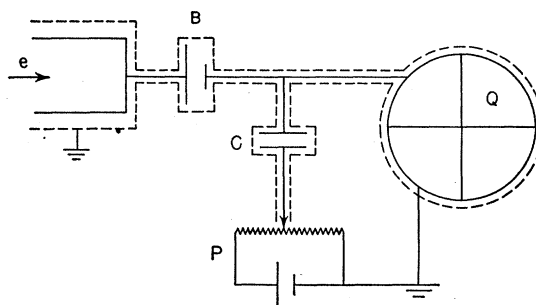


FIG. 8. Diagram for the current-integrating circuit.  $C$  is a polystyrene-insulated capacitor of high leakage resistance.  $B$  is a hearing-aid type battery used only in preliminary tests.  $Q$  is a quadrant electrometer, used as a null indicator.

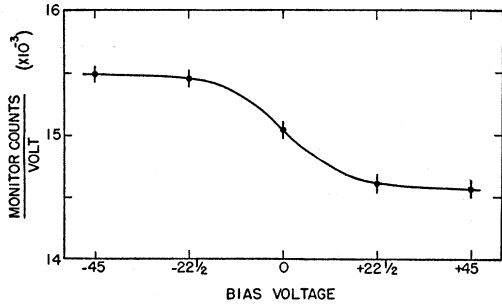


FIG. 9. The ratio (total monitor counts)/(total volts on capacitor) as a function of the bias voltage on the current collection cup. The monitor counts should be independent of the bias voltage, while the volts on the capacitor depend on the different ionization currents at different bias voltages.

## VI. ANALYSIS OF DATA

The recorded data consisted of measurements of the average single and coincidence count rates with the foil in and out of position. Because there are two coincidence pairs for each foil position, there are four sets of data which can be used to determine four desired unknown quantities. The important unknown quantity is the real  $e-e$  coincidence rate due to the scattering foil which gives directly the quantity  $Y$  of Eq. (2). Other unknowns which affect the coincidence measurements are the in and out-of-plane real coincidences, which may be produced by scattering processes in the collimator, and the accidental coincidences. The latter could be predicted from the measured single count average rates were it not for the fact that the accelerator operation is not uniform in time. If the accelerator operation is nearly uniform, it can be shown that the accidental coincidences are determined to close approximation by the average count rates and the average value of  $s^2(t)$ , where  $s(t)$  is the fractional deviation of the beam current at time  $t$  from the average value. The average value,  $\langle s^2 \rangle_{Av}$ , of  $s^2(t)$  is the fourth parameter determined by the data, and with this it becomes possible to make a good approximate solution for  $Y$  of Eq. (2). The necessary approximations involve only these assumptions: (1) the probability of two or more real  $e-e$  or background coincidences per burst of the accelerator is negligible; (2) the average values of powers higher than the second of  $s(t)$  are negligible; and (3) that in many runs the average value of  $s^2(t)$  is the same with the foil in as out. From the data it was determined that these approximations would make errors considerably less than one percent.

Considerable data was evaluated using no other approximations than the three listed above. In practice

it was found useful to combine the four equations predicting observed coincidences as a sum of real and accidental coincidences into the following result, which can be used to illustrate the magnitudes of the count rates and a good approximate method of solution.

$$\begin{aligned} & (n_{13} - n_{36}) - (n_{13}^{\circ} - n_{36}^{\circ}) \\ &= \epsilon_{13}' [1 - (1 + \langle s^2 \rangle_{Av})(n_1 + n_3)] \\ & \quad + (1 + \langle s^2 \rangle_{Av}) [n_3(n_1 - n_6) - n_3^{\circ}(n_1^{\circ} - n_6^{\circ})] \\ & \quad + (1 + \langle s^2 \rangle_{Av}) \epsilon_{13}^{\circ} (n_1^{\circ} + n_3^{\circ} - n_1 - n_3) \\ & \quad - (1 + \langle s^2 \rangle_{Av}) \epsilon_{36}^{\circ} (n_6^{\circ} + n_3^{\circ} - n_3 - n_6). \quad (3) \end{aligned}$$

Equation (3) is written for the case of a measurement at  $\theta^* = 90^\circ$ , where counters 1 and 3 (Fig. 4) are coplanar with the incident beam so as to detect  $e-e$  coincidences. The defining aperture is in front of counter 3, while counters 1 and 6 have larger equal apertures. In Eq. (3) the quantities  $n_1$ ,  $n_3$ ,  $n_6$  represent the measured average count rates in counters 1, 3, and 6 per pulse of the accelerator, with foil in place. The measured average coincidence rates per pulse with foil in are given by  $n_{13}$  and  $n_{36}$ . The corresponding rates with foil out are given by the same symbols with superscript zero. The quantity  $\epsilon_{13}'$  is the unknown to be evaluated which represents the true  $e-e$  coincidence probability per burst of the accelerator, while  $\epsilon_{13}^{\circ}$  and  $\epsilon_{36}^{\circ}$  represent the true coincidence probabilities produced by the background. In forming Eq. (3), large terms containing  $\langle s^2 \rangle_{Av}$  have cancelled out. The most important term on the right-hand side is  $\epsilon_{13}'$  alone. Because of the near equality of  $n_1$  and  $n_6$ , only a small error (less than one percent) is introduced by neglecting  $\langle s^2 \rangle_{Av}$ . The  $\epsilon^{\circ}$  quantities can be determined from the data with the foil out of the beam, and then Eq. (3) can be solved to yield  $\epsilon_{13}$  in terms of experimental quantities.

Table I gives some typical values of the count rates and results observed in the experiment.

It may be noted here that the quantities  $(n_1 - n_1^{\circ})$  and  $(n_6 - n_6^{\circ})$  have the physical significance of being the count rates arising from the foil alone. Ideally, they should be equal, since, in this example, counters 1 and 6 have equal apertures. This was found to be true experimentally, with a standard deviation of about 5 percent, which can be attributed to variations in the accelerator operating conditions. The experimental equality of these rates constitutes an important check on the line-up of the apparatus.

## VII. RESULTS

The results are summarized in Table II. Each line in the table corresponds to some one set of operating

TABLE I. Typical average count rates. (The notation is the same as in the text.)

| $n_1$            | $n_2$            | $n_6$            | $n_{13}$         | $n_{36}$         | $n_1^{\circ}$    | $n_3^{\circ}$    | $n_6^{\circ}$    | $n_{13}^{\circ}$ | $n_{36}^{\circ}$ | $\epsilon_{13}^{\circ}$ | $\epsilon_{36}^{\circ}$ | $\epsilon_{13}'$ |
|------------------|------------------|------------------|------------------|------------------|------------------|------------------|------------------|------------------|------------------|-------------------------|-------------------------|------------------|
| 1.043            | 3.86             | 8.34             | 8.19             | 3.26             | 7.65             | 1.80             | 5.48             | 1.88             | 1.30             | 5.05                    | 3.15                    | 4.43             |
| $\times 10^{-1}$ | $\times 10^{-3}$ | $\times 10^{-2}$ | $\times 10^{-4}$ | $\times 10^{-4}$ | $\times 10^{-2}$ | $\times 10^{-3}$ | $\times 10^{-2}$ | $\times 10^{-4}$ | $\times 10^{-4}$ | $\times 10^{-5}$        | $\times 10^{-5}$        | $\times 10^{-1}$ |

TABLE II. Summary of results.

| Positions and types of counters used          | Position and solid angle of defining aperture            | Solid angle of conjugate aperture (sterad.) | Thickness of Be foil mg/cm <sup>2</sup> | Møller theory $\sigma \times 10^{25}$ cm <sup>2</sup> (sterad.) | Exp. $\sigma$ and percent diff. | Remarks  |
|---|--|---|---|---|---------------------------------|--|
| (1,3,6)<br>Argon-alcohol                      | (3)( $\theta^*=90^\circ$ )<br>$7.15 \times 10^{-4}$      | $5.21 \times 10^{-3}$                       | 0.790                                   | 2.32  | $2.12 \pm 0.08$<br>-8.6%        |  |
| (1,3,6)<br>Argon-alcohol                      | (3)( $\theta^*=90^\circ$ )<br>$7.15 \times 10^{-4}$      | $5.21 \times 10^{-3}$                       | 0.790                                   | 2.32  | $2.07 \pm 0.24$<br>-10.8%       | Large current-integrating capacitor.             |
| (1,3,6)<br>Argon-alcohol                      | (3)( $\theta^*=90^\circ$ )<br>$7.15 \times 10^{-4}$      | $3.31 \times 10^{-3}$                       | 0.790                                   | 2.32  | $1.82 \pm 0.10$<br>-21.6%       | Conjugate aperture made too small intentionally. |
| (1,3,6)<br>Argon-alcohol                      | (3)( $\theta^*=90^\circ$ )<br>$3.68 \times 10^{-4}$      | $5.21 \times 10^{-3}$                       | 0.790                                   | 2.32  | $1.87 \pm 0.18$<br>-19.4%       |  |
| (1,3,6)<br>(3)Argon-alcohol<br>(1,6)Tracerlab | (3)( $\theta^*=90^\circ$ )<br>$7.15 \times 10^{-4}$      | $8.95 \times 10^{-3}$                       | 1.473                                   | 2.32  | $2.05 \pm 0.11$<br>-11.6%       |  |
| (1,3,6)<br>(3)Argon-alcohol<br>(1,6)Tracerlab | (3)( $\theta^*=90^\circ$ )<br>$7.15 \times 10^{-4}$      | $7.25 \times 10^{-3}$                       | 1.473                                   | 2.32  | $2.16 \pm 0.10$<br>-7.1%        |  |
| (1,3,6)<br>Tracerlab                          | (1)( $\theta^*=90^\circ$ )<br>$7.15 \times 10^{-4}$      | $8.95 \times 10^{-3}$                       | 1.473                                   | 2.32  | $2.15 \pm 0.11$<br>-7.3%        |  |
| (1,3,6)<br>Tracerlab                          | (1)( $\theta^*=90^\circ$ )<br>$14.6 \times 10^{-4}$      | $8.95 \times 10^{-3}$                       | 1.473                                   | 2.32  | $2.24 \pm 0.11$<br>-3.5%        |  |
| (2,4,5)<br>Argon-alcohol                      | (4)( $\theta^*=109^\circ 19'$ )<br>$7.98 \times 10^{-4}$ | $5.67 \times 10^{-3}$                       | $\frac{0.790}{\cos 20^\circ}$           | 1.71  | $1.63 \pm 0.10$<br>-4.4%        |  |

conditions, which are indicated in the first four columns and in the column headed "Remarks."

The probable errors indicated in column 6 are the expected standard deviations computed solely on the basis of the number of counts recorded. Possible systematic errors will be discussed below.

Line 2 in the table gives the result obtained when two 0.001-microfarad condensers were used in parallel, in place of the usual one, in the current integrating circuit. This was done to check for the possibility of gross errors in the current measurement.

For the case given in line 3, the conjugate aperture was deliberately made smaller than the minimum size demanded by calculations. As was expected, the result was lower in this case, by an amount which agreed with estimates of the effects of plural scattering in the foil.

The points obtained under various conditions at  $\theta^*=90$  degrees are plotted in Fig. 10 as a function of the difference between the conjugate aperture diameter and the defining aperture diameter. The expected influence of plural scattering is shown by the dashed curve which was computed numerically using the multiple scattering theory of Snyder and Scott,<sup>10</sup> and taking into account the finite size and divergence of the incident beam. The dashed curve was normalized to yield the Møller cross section at large values of the conjugate aperture. Within the statistical accuracy of the data, the experimental points would fit a curve lying parallel to the dashed curve. The numerical calculations are thus supported by the data in indicating that the loss due to plural scattering is very

small for those experiments where the larger conjugate apertures were used.

The expected standard deviation in the result at  $\theta^*=109$  degrees (line 9) was not made less than  $\pm 6$  percent because the time required for this would have been excessive.

The quantity  $\sigma$  is the cross section (per electron) per unit solid angle. Theoretical values were calculated from Eq. (1).

### VIII. DISCUSSION

The weighted average of the results at  $\theta^*=90$  degrees (excluding lines 2 and 3 of Table II) is  $2.13 \pm 0.043$ . This is about 8 percent lower than the Møller value, with an expected standard deviation from statistics alone of  $\pm 2$  percent. At  $\theta^*=109$  degrees 19 minutes, the experimental result is 4.4 percent too low, with an expected standard deviation of  $\pm 6$  percent. A similar comparison with the Mott formula<sup>2</sup> shows the experimental results to be about 90 percent higher at 90 degrees and 65 percent higher at 109 degrees than the Mott formula predicts. Our result is thus in agreement with other experiments,<sup>5,6</sup> conducted with different energy electrons, in supporting the Møller formula.

Most of the points at which systematic errors may have been introduced have been discussed above. Our estimate of the expected maximum values of the chief possible errors, together with the direction in which they would be expected to affect the experimental result, may be summarized as follows: (1) Geiger counter efficiency, +0, -3 percent; (2) foil thickness,  $\pm 2$  percent; (3) integration of electron current,  $\pm 2$  percent; (4) inadequate conjugate aperture size (excluding radiative effects), +0, -1 percent; (5) error in

<sup>10</sup> H. S. Snyder and W. T. Scott, Phys. Rev. **76**, 220 (1949).

incident electron energy,  $\pm 2$  percent; (6) uncertainty in defining aperture size because of leakage effects,  $+1$ ,  $-0$  percent; (7) approximations in calculations,  $\pm 1$  percent. It may be seen that an unfortunate combination of these errors could make the experimental result as much as 8 percent too low. However, we believe that these estimates are conservative, and that a systematic error greater than 5 percent is unlikely. With the view, the experiment leaves room for a discrepancy between theory and experiment.

The Møller theory did not take into account the radiative effects accompanying an  $e-e$  event. Heitler<sup>11</sup> has shown that the order of magnitude of the real radiation is given by the Bethe-Heitler bremsstrahlung formula. Lanzl and Hanson<sup>12</sup> find experimental support for this conclusion. Therefore it is to be expected that in some of the  $e-e$  events an appreciable fraction of the energy will be carried off by a photon, and the angular correlation, essential for the coincidence technique, will be destroyed. However, some allowance can be made for such de-correlation by increasing the size of the conjugate aperture. The larger conjugate apertures used in the present experiment were large enough to catch both electrons, even though a photon carried off an energy of approximately 100 keV. Numerical calculations of the probability that photons of this energy or greater be radiated in a 6-MeV  $e-e$  collision are not available as yet. In the corresponding case of an  $e-p$  collision the probability is the order of several percent for those collisions where the electron suffers large deflections. The purely quantum electrodynamic radiative correction for  $e-e$  scattering has been calculated by Lomanitz,<sup>13</sup> and its magnitude is probably considerably less than one percent.<sup>14</sup> The radiative effects are thus due to the emission of real quanta. They are in the correct direction to account for the difference between the Møller theory and experiment, and it is not improbable that they are of sufficient magnitude.

<sup>11</sup> W. Heitler, *Quantum Theory of Radiation* (Oxford University Press, London, 1947), second edition, Appendix.

<sup>12</sup> L. H. Lanzl and A. O. Hanson, *Phys. Rev.* **83**, 959 (1951).

<sup>13</sup> R. Lomanitz, thesis, Dept. of Physics, Cornell University (unpublished).

<sup>14</sup> H. A. Bethe (private communication).

In addition to radiation there are other effects which might produce a discrepancy between Møller theory and experiment. For example, the Møller theory applies to free electrons, whereas in any experiment some of the target electrons are near the nucleus. Small effects due to interference with nuclear scattering should therefore be expected.

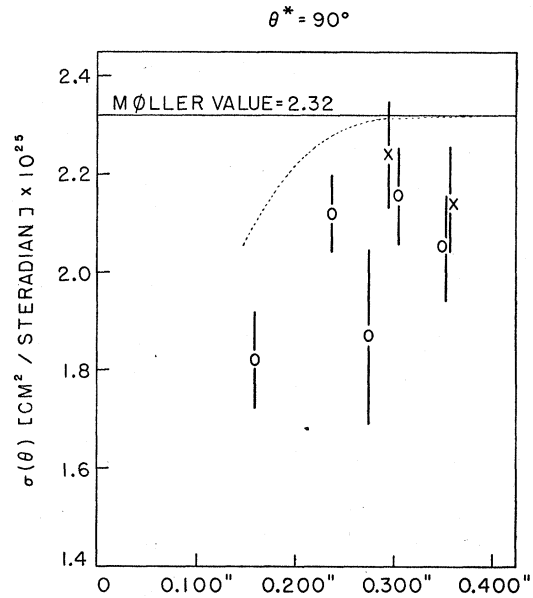


FIG. 10. Observed values of the absolute differential cross section as a function of the difference between the conjugate aperture diameter and the defining aperture diameter. This difference is a measure of the allowance made for the effects of multiple scattering and possible misalignment. The dashed curve gives a theoretical result for the expected loss due to multiple scattering. The theoretical curve has been normalized to give the Møller cross section at large aperture differences.

In closing, we should like to point out that recent results obtained elsewhere<sup>5,6</sup> on  $e-e$  scattering are also a few percent lower than the Møller theory predicts. In one of these cases,<sup>6</sup> the authors mention the possibility that systematic errors could account for the difference.

We are indebted to Mr. R. Torres, who built and tested some of the electronic components and to Mr. D. A. Caswell, who assisted in some of the early design work.

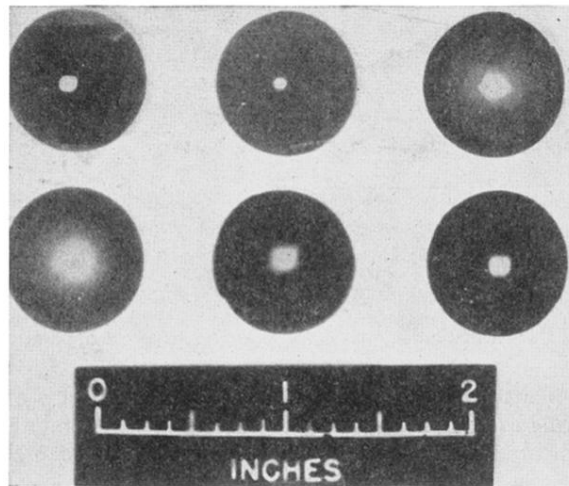


FIG. 3. Cross sections of the electron beam at various points along its path. Upper row from right to left: (1) At the entrance to the collimator tube. The horizontal spread results from the spread in energy of the electrons from the accelerator. (2) At the exit of the collimator tube. (3) At the position of the scattering foil. Lower row from right to left: (1) At the end of the exit tube of the scattering chamber. (2) At a point 4 inches in front of the collection cup. (3) Same position as for (2), but with a  $\frac{1}{4}$ -mil nylon foil scatterer.